Engineering photon statistics in a spinor polariton condensate: Supplemental Information

S. Baryshev,[1] A. Zasedatelev,[2,1,*] H. Sigurdsson,[3,2] I. Gnusov,[1]
J. D. Töpfer,[2] A. Askitopoulos,[1] and P. G. Lagoudakis[1,2]

[1]*Hybrid Photonics Laboratory, Skolkovo Institute of Science and Technology, Territory of Innovation Center Skolkovo, 6 Bolshoy Boulevard 30, building 1, 121205 Moscow, Russia*
[2]*School of Physics and Astronomy, University of Southampton, Southampton, SO17 1BJ, UK.*
[3]*Science Institute, University of Iceland, Dunhagi 3, IS-107, Reykjavik, Iceland*

I. POLARIZATION SWITCHING AND PINNING

In this section we present additional data regarding the non-trivial spinor dynamics of a polariton condensate. We implement polarization resolved time series analysis and integrated polarimetry measurements. We measure all the Stokes parameters and calculate the degree of polarization, defined as DOP $= \sqrt{S_1^2 + S_2^2 + S_3^2}$, of the cavity emitted light, to further support findings discussed in this letter. When the condensate is pumped with linearly polarized light and experiences finite cavity birefringence which is quantified in terms of an effective in-plane magnetic field $\mathbf{\Omega}_\parallel$, polarization pinning is observed which causes the condensate to emit photons with linear polarization dominantly parallel to $\mathbf{\Omega}_\parallel$ [1].

In Fig. S1 we show the polarization resolved 1 μs long time series of condensate emission at $P = 1.6P_{th}$. While the mean condensate polarization is dominantly pinned to the vertical projection, we observe abrupt and completely random in time condensate emission polarization switching events (indicated by green shaded areas). This type of behavior is present in many pulses (not shown here) and number of switching events is random within the pulse.

As discussed in the letter, emergence of finite cavity birefringence and the effective in-plane magnetic field $\mathbf{\Omega}_\parallel$ is location sensitive. Hence, in Fig. S2 we present $g^{(2)}_{H,H}(\tau)$, $g^{(2)}_{V,V}(\tau)$ and $g^{(2)}_{H,V}(\tau)$ data taken from the different point on the sample at $P = 1.48P_{th}$. One may notice that the amplitude of the bunching, $g^{(2)}_{i,i}(0)$, is different from what is presented in the Fig. 3(a) of the main text for the same power. In Fig. S3(a) we show power dependence for the $g^{(2)}_{H,H}(0)$ and $g^{(2)}_{V,V}(0)$, similar to what we present in Fig. 3(a) in the letter text. We note that the measurements in Figs. S2 and S3 are performed at a different sample location than those in Figs. 2-3 and 4-5 in the main text which is the reason for some quantitative, but not qualitative differences.

As long as a finite birefringent field exists $\mathbf{\Omega}_\parallel$ then one can expect the nonlinearity of the condensate dynamics to pin the pseudospin parallel to this field. The results in Fig. S3(a) indicate the expected behavior with power, i.e. decrease of $g^{(2)}_{V,V}(0)$ (red circles) to unity for $P > 1.35P_{th}$ as more polaritons in the condensate become vertically polarized while $g^{(2)}_{H,H}(0)$ (black circles) increases. Imposed onto the plot, in green triangles, is the S_1 Stokes component power dependence which shows how one of the polarizations (vertical, in our case) becomes dominant in the system. From the measured DOP in Fig. S3(b) we can see that the emitted condensate light, right after the condensation threshold, is unpolarized and starts to become polarized after $P = 1.35P_{th}$ when the pinning effect kicks in [1].

II. DYNAMICAL MEAN FIELD EQUATIONS

The dynamics of the spinor polariton condensate order parameter is modeled through a set of stochastic driven-dissipative Gross-Pitaevskii equations (Langevin type equations) coupled to spin-polarized rate equations describing excitonic reservoirs $X_\pm$ feeding the two spin components $\psi_\pm$ of the condensate. The stochastic part of our model ($\theta_\pm$) was formulated in Refs. [2, 3] in the truncated Wigner approximation which becomes valid above condensation threshold with large particle numbers in the condensate $\langle n \rangle \gg 1$ such that stimulated effects dominate over spontaneous scattering events. We point out that a more accurate treatment of dissipative many-body quantum systems involves writing a density matrix for the polariton field governed by appropriate master equations [4]. This approach is beyond

* A.Zasedatelev@skoltech.ru

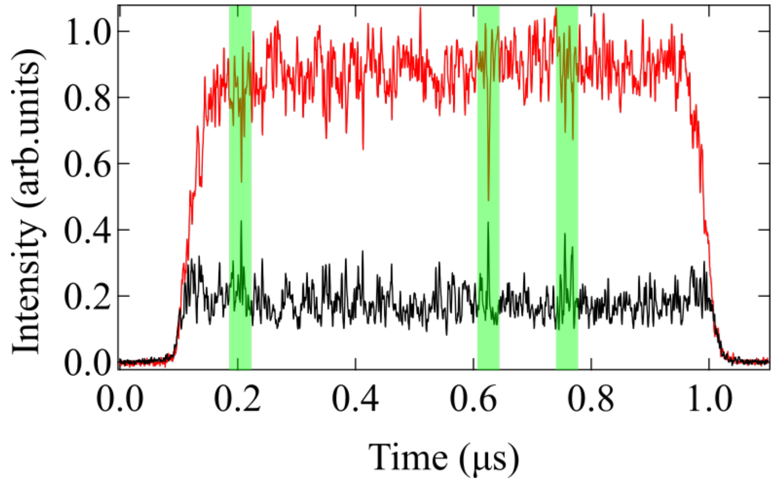

Figure S1. Measured time series (1 μs excitation pulse) for condensate H (black) and V (red) polarized emission. Here, we observe switching (highlighted with pale green rectangles) of intensity between the polarizations which contribute to the large values of $g^{(2)}_{H,H}(0)$.

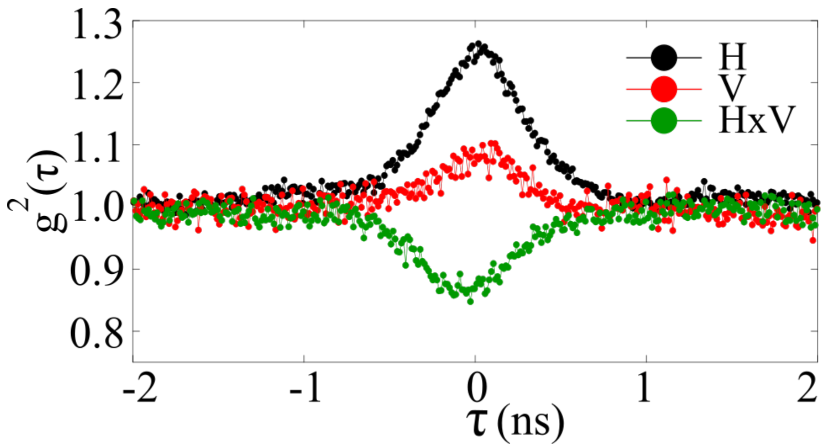

Figure S2. Second order correlation function of the condensate, measured with polarization filtering at $P = 1.48P_{th}$. $g^{(2)}_{H,H}(\tau)$ (black), $g^{(2)}_{V,V}(\tau)$ (red), and $g^{(2)}_{H,V}(\tau)$ (green).

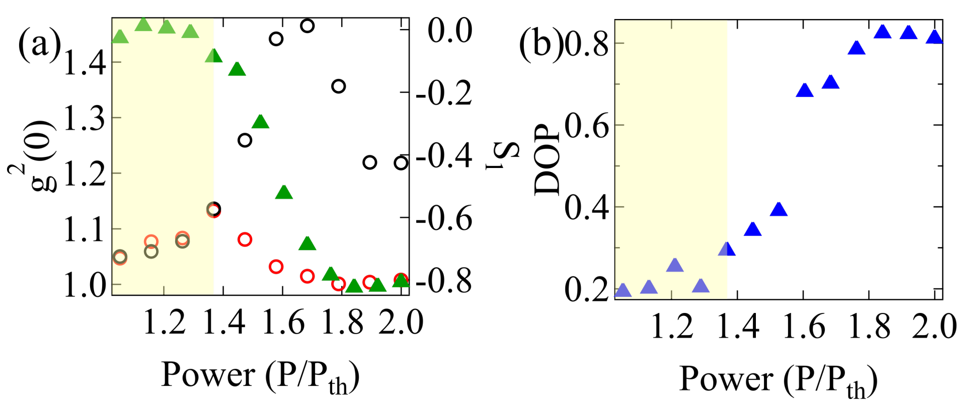

Figure S3. (a) Experimentally measured $g^{(2)}_{H,H}(0)$ (black circles) and $g^{(2)}_{V,V}(0)$ (red circles) power dependence and corresponding time-integrated S_1 component (green triangles). (b) Corresponding power dependence of the condensate DOP. Pale yellow background highlights the pump power range without polarization pinning (low DOP).

the scope of the current study where our modelling concerns the limit of large particle numbers where we show that complex nonlinear mean-field forces have quite dramatic effects on the emitted photon statistics. The model reads:

$$i\frac{d\psi_\sigma}{dt} = \frac{1}{2}\Big[\nu V_\sigma + i\left(R_1 X_\sigma + R_2 X_{-\sigma} - \Gamma\right)\Big]\psi_\sigma - \nu\frac{\Omega_x}{2}\psi_{-\sigma} + \theta_\sigma(t), \tag{1a}$$

$$\frac{dX_\sigma}{dt} = -\left[\Gamma_R + R_1(|\psi_\sigma|^2+1) + R_2(|\psi_{-\sigma}|^2+1)\right]X_\sigma + \Gamma_s(X_{-\sigma} - X_\sigma) + P_\sigma, \tag{1b}$$

$$V_\sigma = \alpha_1|\psi_\sigma|^2 + \alpha_2|\psi_{-\sigma}|^2 + g_1\left(X_\sigma + \frac{P_\sigma}{W}\right) + g_2\left(X_{-\sigma} + \frac{P_{-\sigma}}{W}\right). \tag{1c}$$

Here, $\sigma \in \{+,-\}$ are the two spin indices, $\alpha_{1,2}$ denotes the same-spin (triplet) and opposite-spin (singlet) polariton-polariton interaction strengths and $g_{1,2}$ are the corresponding interactions with the reservoir, $R_{1,2}$ is the rate of stimulated same-spin and opposite-spin scattering of polaritons into the condensate, and Γ is the polariton decay rate, Γ_R and Γ_s describe the decay rate and spin relaxation of reservoir excitons. In principle, scattering from the reservoirs to the condensate should be dominantly spin-preserving (R_1) but in the presence of a (effective) magnetic field (Ω_x) one needs to account for the possibility that particles from the opposite-spin reservoir can scatter (R_2) into the condensate [5, 6]. Some studies work under the approximation that in optical traps the condensate is so well separated from the background reservoir and that blueshift coming from polariton-exciton interactions can be discarded but recent studies [7] have shown that the reservoir is actually not so distant from the condensate and therefore additional polariton condensate blueshift coming from this background reservoir ($g_{1,2}$) should be taken into account. For all results presented we have chosen $\alpha_2 = -0.2\alpha_1$ and $g_2 = -0.2g_1$ [8]. We also include an energy dampening parameter $\nu = 1 - i\nu'$ according to the Landau-Khalatnikov approach [2]. Finally, spin-mixing (spin-relaxation) between the reservoirs (Γ_s) should be taken into account as it can be evidenced as depolarization in the cavity photoluminescence below condensation threshold [9–14]. It is naturally quite challenging to understand the full picture of which parameters contribute to different observed effects in experiment and thus we attempt at being as inclusive as possible of different physical mechanisms.

Although the experiment deals with a birefringent field $\mathbf{\Omega}_\parallel = (\Omega_x, \Omega_y)^T$ at a specific angle we will, without any loss of generality, take the splitting to be between horizontal $\psi_H = (\psi_+ + \psi_-)/\sqrt{2}$ and vertical $\psi_V = (\psi_+ - \psi_-)/\sqrt{2}$ polarized modes represented by $\Omega_x > 0$ and $\Omega_y = 0$. The strength of the white complex-valued noise $\theta_\sigma(t)$ is determined by the scattering rate of polaritons into the condensate,

$$\langle \theta_\sigma(t)\theta_{\sigma'}(t')\rangle = 0, \qquad \langle \theta_\sigma(t)\theta^*_{\sigma'}(t')\rangle = \frac{R_1 X_\sigma + R_2 X_{-\sigma}}{2}\delta_{\sigma\sigma'}\delta(t-t'). \tag{2}$$

The active reservoir X_σ, which feeds the condensate with particles, is driven by a background of high momentum *inactive* excitons P_σ which do not satisfy energy-momentum conservation rules to scatter into the condensate. Assuming the simplest type of rate equation describing the conversion of optical excitation power into an inactive reservoir in the continuous wave regime we write:

$$\frac{dP_\sigma}{dt} = -(W + \Gamma_I)P_\sigma + \Gamma_s(P_{-\sigma} - P_\sigma) + L_\sigma. \tag{3}$$

Here, W is a phenomenological spin-conserving redistribution rate of inactive excitons into active excitons and Γ_I is the nonradiative exciton decay rate. Since these inactive excitons also experience spin relaxation Γ_s the polarization of P_σ will not coincide with that of the incident optical excitation. As the experiment is performed in the continuous-wave regime we can immediately solve the steady state solution of Eq. (3) and plug it into Eqs. (1). For optical excitation parameterized as $\mathbf{L} = L(\cos^2(\Theta), \sin^2(\Theta))^T$ where L is the power of the optical excitation and Θ can be understood as a quarter waveplate angle in the experimental setup which determines the polarization of the incident light, we can write the background inactive reservoir as,

$$\begin{pmatrix} P_+ \\ P_- \end{pmatrix} = \frac{L}{W + 2\Gamma_s}\begin{pmatrix} W\cos^2(\Theta) + \Gamma_s \\ W\sin^2(\Theta) + \Gamma_s \end{pmatrix}. \tag{4}$$

Here, we have neglected Γ_I since we assume nonradiative losses are much slower than the redistribution rate of excitons $W \gg \Gamma_I$.

Determining the parameters of Eq. (1) poses a challenge since they will depend in a complicated way on both sample and excitation properties. To overcome this, we implement a random walk algorithm which, in each step, calculates the root-mean-square-error between the data from experiment and simulation. The algorithm starts from a random set of parameters (appropriately bounded to remain physical) and repeatedly takes a random step forward in parameter space which is kept if the error is lowered. If the error rises, the step is discarded (go back to previous step) and a new random step is tested. Performing 500 random initializations in the parameter space, with each taking 300 random steps, we determine a set of parameters best fitting the experimental results. The parameters used throughout the manuscript are given in units of Γ except of ν' which is dimensionless: $\Gamma_R = 1.6$; $\Gamma_s = 0.19$; $W = 0.156$; $R_1 = 0.0032$; $R_2 = 0.0027$; $\alpha_1 = 0.00015$; $g_1 = 0.00097$; $\nu' = 0.077$. For Fig. 3(a) and 5(c,d) in the main text we have set $\Omega_x = -0.057$ and -0.0072 respectively as they correspond to different sample locations. The theoretical pump threshold value for linearly polarized excitation corresponds to a threshold laser power L defined as $P_{th} = P_\pm(L_{th})$,

$$L_{th} = \frac{2\Gamma\Gamma_R}{R_1 + R_2 + \nu'(g_1 + g_2)(1 + \Gamma_R/W)}. \tag{5}$$

III. INFLUENCE OF RESIDUAL ELLIPTICITY

In this section we investigate the effects of small detrimental ellipticity in the excitation laser and how it affects our results presented in Fig. 3 in the main manuscript. In Fig. S4(a) we show the calculated zero time delay second order correlation functions between the linear polarization components (horizontal and vertical specifically) averaged over 100 different realizations of the condensate (i.e., Monte-Carlo sampling) where each realization is integrated over 10 ns. The whole lines are the same as in Fig. 3(a) in the main text corresponding to a linearly polarized excitation $\Theta = 45°$ whereas the dashed lines represent simulation with a slight ellipticity $\Theta = 46°$ (or alternatively, QWP angle of 1°). The circle markers are experimental data. In Fig. S4(b) we show the corresponding time-integrated pseudospin components. As expected, for a finite elliptcty we see that circular polarization builds up with growing power due to the power-dependent spin imbalance increasing in the reservoirs which provides differential gain and blueshift to the spins $\psi_\pm$. The increase of the condensate circular polarization S_3 is accompanied by a decrease in the vertical linear polarization (i.e., S_1 becomes less negative) which results in reduction of the $g^{(2)}_{H,H}(0)$ as evident from the black dashed line in Fig. S2(a).

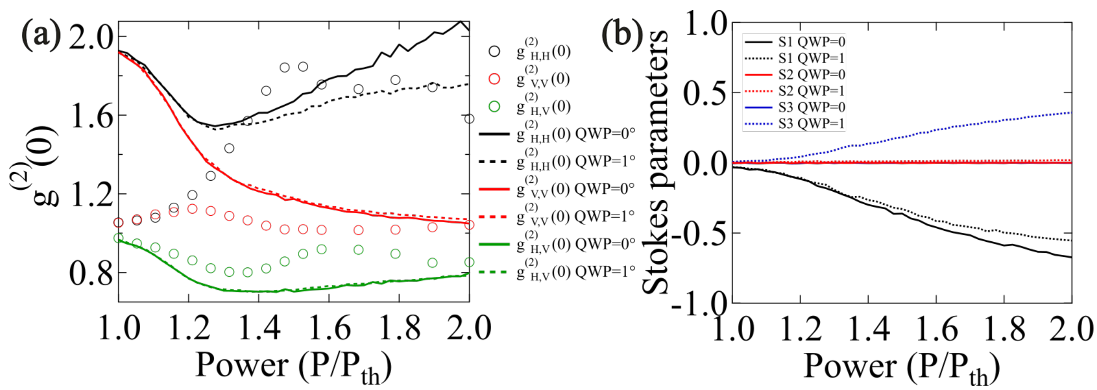

Figure S4. (a) $g^{(2)}_{H,H}(0)$ (black), $g^{(2)}_{V,V}(0)$ (red) and $g^{(2)}_{H,V}(0)$ (green) power dependencies. Experimentally measured (circles) and theoretically obtained data with purely linearly polarized excitation (solid line) and with slightly elliptically polarized excitation (dashed line). (b) Theoretically obtained time integrated pseudospin parameters with purely linearly (solid line) polarized excitation and slightly elliptical (dashed line) excitation polarization.

[1] I. Gnusov, H. Sigurdsson, S. Baryshev, T. Ermatov, A. Askitopoulos, and P. G. Lagoudakis, Optical orientation, polarization pinning, and depolarization dynamics in optically confined polariton condensates, Phys. Rev. B **102**, 125419 (2020).

[2] D. Read, T. C. H. Liew, Y. G. Rubo, and A. V. Kavokin, Stochastic polarization formation in exciton-polariton Bose-Einstein condensates, Phys. Rev. B **80**, 195309 (2009).

[3] M. Wouters and V. Savona, Stochastic classical field model for polariton condensates, Phys. Rev. B **79**, 165302 (2009).

[4] E. Del Valle, *Microcavity Quantum Electrodynamics* (VDM, Saarbrücken, 2010).

[5] D. D. Solnyshkov, I. A. Shelykh, M. M. Glazov, G. Malpuech, T. Amand, P. Renucci, X. Marie, and A. V. Kavokin, Nonlinear effects in spin relaxation of cavity polaritons, Semiconductors **41**, 1080 (2007).

[6] Y. del Valle-Inclan Redondo, H. Ohadi, Y. G. Rubo, O. Beer, A. J. Ramsay, S. I. Tsintzos, Z. Hatzopoulos, P. G. Savvidis, and J. J. Baumberg, Stochastic spin flips in polariton condensates: nonlinear tuning from GHz to sub-Hz, New Journal of Physics **20**, 075008 (2018).

[7] M. Boozarjmehr, M. Steger, K. West, L. N. Pfeiffer, D. W. Snoke, A. G. Truscott, E. A. Ostrovskaya, and M. Pieczarka, Spatial distribution of an optically induced excitonic reservoir below exciton-polariton condensation threshold (2020), arXiv:1912.07765 [cond-mat.quant-gas].

[8] C. Ciuti, V. Savona, C. Piermarocchi, A. Quattropani, and P. Schwendimann, Role of the exchange of carriers in elastic exciton-exciton scattering in quantum wells, Phys. Rev. B **58**, 7926 (1998).

[9] M. Z. Maialle, E. A. de Andrada e Silva, and L. J. Sham, Exciton spin dynamics in quantum wells, Phys. Rev. B **47**, 15776 (1993).

[10] L. Viña, Spin relaxation in low-dimensional systems, Journal of Physics: Condensed Matter **11**, 5929 (1999).

[11] H. Ohadi, E. Kammann, T. C. H. Liew, K. G. Lagoudakis, A. V. Kavokin, and P. G. Lagoudakis, Spontaneous symmetry breaking in a polariton and photon laser, Phys. Rev. Lett. **109**, 016404 (2012).

[12] Y. del Valle-Inclan Redondo, H. Sigurdsson, H. Ohadi, I. A. Shelykh, Y. G. Rubo, Z. Hatzopoulos, P. G. Savvidis, and J. J. Baumberg, Observation of inversion, hysteresis, and collapse of spin in optically trapped polariton condensates, Phys. Rev. B **99**, 165311 (2019).

[13] M. Klaas, O. A. Egorov, T. C. H. Liew, A. Nalitov, V. Marković, H. Suchomel, T. H. Harder, S. Betzold, E. A. Ostrovskaya, A. Kavokin, S. Klembt, S. Höfling, and C. Schneider, Nonresonant spin selection methods and polarization control in exciton-polariton condensates, Phys. Rev. B **99**, 115303 (2019).

[14] L. Pickup, J. D. Töpfer, H. Sigurdsson, and P. G. Lagoudakis, Polariton spin jets through optical control, Phys. Rev. B **103**, 155302 (2021).